epl draft

Stability of jammed packings II: the transverse length scale

S. S. Schoenholz[1], C. P. Goodrich[1], O. Kogan[1,2], A. J. Liu[1] and S. R. Nagel[2]

[1] *Department of Physics, University of Pennsylvania, Philadelphia, Pennsylvania 19104, USA*
[2] *James Franck and Enrico Fermi Institutes and Department of Physics, The University of Chicago, Chicago, Illinois 60637, USA*

PACS 62.20.M- – Structural failure of materials
PACS 63.50.Lm – (Vibrational states in disordered materials) Glasses and amorphous solids
PACS 63.70.+h – Statistical mechanics of lattice vibrations and displacive phase transitions

Abstract – At zero temperature and applied stress, an amorphous packing of spheres exhibits, as a function of packing fraction, a jamming transition where the system is sensitive to boundary conditions even in the thermodynamic limit. Upon further compression, the system should become insensitive to boundary conditions but only if it is sufficiently large. Here we explore the linear response to a large class of boundary perturbations in 2 and 3 dimensions. We consider each finite packing with periodic-boundary conditions as the basis of an infinite square or cubic lattice and study properties of vibrational modes at arbitrary wave vector. Our results can be understood in terms of competition between plane waves and the anomalous vibrational modes associated with the jamming transition; boundary perturbations become irrelevant for systems that are larger than a previously identified transverse length that diverges at the jamming transition.

Introduction. – At the jamming transition of ideal spheres, the removal of a single contact causes the previously rigid system to become mechanically unstable and crumble [1–3]. Thus at the transition, the replacement of periodic-boundary conditions with free-boundary conditions destroys rigidity even in the thermodynamic limit [4–6]. Recognizing that packings at the jamming threshold are susceptible to boundary conditions, Torquato and Stillinger [7] drew a distinction between collectively jammed packings, which are stable when the confining box is not allowed to deform, and strictly jammed packings, which are stable to arbitrary perturbations of the boundary. Indeed, infinitesimal changes in the shape of the boundary that leave the contact network invariant can make a difference; Dagois-Bohy *et al.* [8] have shown that jammed packings with periodic-boundary conditions can be linearly unstable to shearing the box.

At densities greater than the jamming transition there are more contacts than the minimum required for stability [1,2]. In this regime one would expect packings that are sufficiently large to be stable to changes in the boundary. How does the characteristic size for a stable system depend on proximity to the jamming transition? The finite-size scaling of quantities such as the contact number [3] is governed not by the linear system size, L, but by the total number of particles in the system, $N = L^d$, for dimension $d \geq 2$; such scaling is expected for systems at or above their upper critical dimension. In contrast, the sensitivity to free- versus periodic-boundary conditions is governed by a length scale, ℓ^*, that diverges at jamming transition. For $L \gg \ell^*$, the system is stable even with free boundaries [4–6].

In this paper, we show that stability for a large class of boundary perturbations is governed by a separate length scale, ℓ_{T}, that also diverges at the jamming transition. Packings with $L \gg \ell_{\mathrm{T}}$ are linearly stable with respect to these boundary perturbations. We understand this as a competition between jamming transition physics at low pressures/system sizes, and transverse acoustic wave physics at high pressures/system sizes. The two lengths, ℓ^* and ℓ_{T}, are the same as the longitudinal and transverse lengths associated with the normal modes of jammed sphere packings [9].

We analyze systems with periodic boundary conditions composed of equal numbers of small and large spheres with diameter ratio 1:1.4 all with equal mass, m. The particles interact via the repulsive finite-range harmonic pair potential

$$V(r_{ij}) = \frac{\varepsilon}{2}\left(1 - \frac{r_{ij}}{\sigma_{ij}}\right)^2 \qquad (1)$$

if $r_{ij} < \sigma_{ij}$ and $V(r_{ij}) = 0$ otherwise. Here r_{ij} is the distance between particles i and j, σ_{ij} is the sum of the

particles' radii, and ε determines the strength of the potential. Energies are measured in units of ε, distances in units of the average particle diameter σ, and frequencies in units of $\sqrt{\varepsilon/m\sigma^2}$. We varied the total number of particles from $N = 32$ to $N = 512$ at 36 pressures between $p = 10^{-1}$ and $p = 10^{-8}$. Particles are initially placed at random in an infinite temperature, $T = \infty$, configuration and are then quenched to a $T = 0$ inherent structure using a combination of linesearch methods, Newtons method and the FIRE algorithm [10]. The resulting packing is then compressed or expanded uniformly in small increments until a target pressure, p, is attained. After each increment of p, the system is again quenched to $T = 0$.

Symmetry-breaking perturbations. – The boundary conditions can be perturbed in a number of ways. The dramatic change from periodic to free boundaries has been studied in refs. [4–6]. Dagois-Bohy *et al.* [8] considered infinitesimal "shear-type" deformations to the *shape* of the periodic box, such as uniaxial compression, shear, dilation, etc. Here, we relax the periodic boundary conditions by considering a third class of perturbations that allow particle displacements that violate periodicity. To do this, we treat our system with periodic boundary conditions as a tiling of identical copies of the system over all space. Thus, an N-particle packing in a box of linear size L with periodic boundary conditions can be viewed as the N-particle unit cell of an infinite hypercubic lattice.

We assume the particles begin in mechanical equilibrium at positions specified by $\boldsymbol{r}^0_{i\mu}$, where i indexes particles in each cell and μ indexes unit cells, so that $\boldsymbol{r}^0_{i\mu}$ is the equilibrium position of particle i in cell μ. The energy of the system to lowest order in particle displacements about its minimum value, $\boldsymbol{u}_{i\mu} = \boldsymbol{r}_{i\mu} - \boldsymbol{r}^0_{i\mu}$, can generically be written as,

$$U = \sum_{\langle i\mu,j\nu\rangle} V(r_{i\mu j\nu}) \sim U_0 + \sum_{\langle i\mu,j\nu\rangle} \boldsymbol{u}^{\mathrm{T}}_{i\mu} \frac{\partial^2 U}{\partial \boldsymbol{r}_{i\mu}\partial \boldsymbol{r}_{j\nu}}\bigg|_{\boldsymbol{r}=\boldsymbol{r}^0} \boldsymbol{u}_{j\nu}, \tag{2}$$

where the sums are over all pairs of particles $i\mu$ and $j\nu$ that are in contact. The equations of motion resulting from eq. (2) can be solved by a plane-wave ansatz, $\boldsymbol{u}_{i\mu} = \mathrm{Re}\{\boldsymbol{\epsilon}_i \exp[i(\boldsymbol{k}\cdot\boldsymbol{R}_\mu - \omega t)]\}$. Here $\boldsymbol{\epsilon}_i$ is a dN-dimensional polarization vector, $\boldsymbol{k}$ is a d-dimensional wavevector and $\boldsymbol{R}_\mu$ is the d-dimensional vector corresponding to the position of cell μ. This gives the eigenvalue equation,

$$\lambda_n(\boldsymbol{k})\boldsymbol{\epsilon}_{ni}(\boldsymbol{k}) = \sum_j \boldsymbol{D}_{ij}(\boldsymbol{k})\boldsymbol{\epsilon}_{nj}(\boldsymbol{k}) \tag{3}$$

where,

$$\boldsymbol{D}_{ij}(\boldsymbol{k}) = \sum_{\mu\nu} \frac{\partial^2 U}{\partial \boldsymbol{r}_{i\mu}\partial \boldsymbol{r}_{j\nu}}\bigg|_{\boldsymbol{r}=\boldsymbol{r}^0} e^{i\boldsymbol{k}\cdot(\boldsymbol{R}_\mu - \boldsymbol{R}_\nu)} \tag{4}$$

is the dynamical matrix of dimension $dN \times dN$, and n labels the eigenvalues and eigenvectors. From eq. (2), the frequency of the modes in the nth branch are $\omega_n(\boldsymbol{k}) = \sqrt{\lambda_n(\boldsymbol{k})}$ with eigenvector $\boldsymbol{\epsilon}_{ni}(\boldsymbol{k})$. Note that when $\boldsymbol{k} = 0$ we recover the normal modes for a system with periodic boundary conditions that have been widely studied [9,11].

With $\boldsymbol{k}$ allowed to vary over the first Brillouin zone, the eigenvectors comprise a complete set of states for the entire tiled system. It follows that any displacement of particles at the boundary of the unit cell can be written as a Fourier series,

$$\boldsymbol{u}_{i\mu} = \sum_{\boldsymbol{k},n} A_{\boldsymbol{k},n}\boldsymbol{\epsilon}_{ni}(\boldsymbol{k}) \exp[i(\boldsymbol{k}\cdot\boldsymbol{R}_\mu)]\,. \tag{5}$$

Therefore, the system will be unstable to some collective perturbation of its boundary if and only if there is some $\boldsymbol{k}$ and n for which $\lambda_n(\boldsymbol{k}) \le 0$. This procedure allows us to characterize boundary perturbations by wavevector.[1] If we find a wavevector whose dynamical matrix has a negative eigenvalue, it follows that the system must be unstable with respect to the boundary perturbation implied by the corresponding eigenvector.

Our aim is to identify the range of system pressures and sizes over which the system is likely to be unstable. This amounts to finding the conditions where the lowest eigenvalue of the sphere packing is likely to be negative. We first consider the so-called "unstressed system," which replaces the original system of spheres with an identical configuration of particles connected by unstretched springs with stiffness given by the original bonds. We will construct scaling relations for the lowest eigenvalue of the unstressed system as well as for the accompanying shift in the eigenvalues upon reintroducing the stress. By finding the pressures and system sizes where these two quantities are comparable, we will thus determine the scaling of the susceptibility of packings to perturbations described by eq. (5).

The unstressed system. – The dynamical matrix in eq. (4) is a function of the second derivative of the pair potentials of eq. (1) with respect to particle positions. To construct the dynamical matrix of the unstressed system, we rewrite this as as

$$\frac{\partial^2 V}{\partial r_\alpha \partial r_\beta} = \frac{\partial^2 V}{\partial r^2}\frac{\partial r}{\partial r_\alpha}\frac{\partial r}{\partial r_\beta} + \frac{\partial V}{\partial r}\frac{\partial^2 r}{\partial r_\alpha \partial r_\beta}, \tag{6}$$

where V is the potential between particles $i\mu$ and $j\nu$, $\boldsymbol{r} \equiv \boldsymbol{r}_{j\nu} - \boldsymbol{r}_{i\mu}$ and α and β are spatial indices. The second term is proportional to the negative of the force between particles. If this term is neglected, there are no repulsive forces and the system will be "unstressed" [5,12]. The dynamical matrix of the unstressed system, obtained from *just* the first term in eq. (6), has only non-negative eigenvalues because it represents a system of unstretched

[1] Note that shear-type deformations can be considered concurrently with the addition of the term $\Lambda\cdot\boldsymbol{r}^0_{i\mu}$ to eq. (5), where Λ is a global deformation tensor. This term represents the affine displacement and is neglected for our purposes.

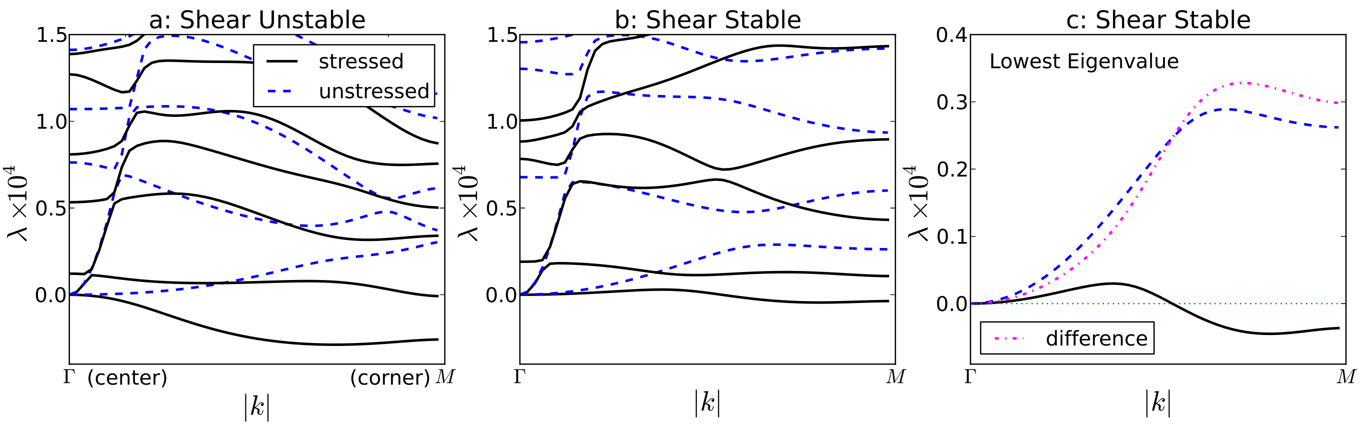

Fig. 1: Dispersion relations along the $\Gamma - M$ line for the lowest few branches of 2 different 2-dimensional packings of $N = 1024$ particles. The Γ point is at the Brillouin zone center ($\boldsymbol{k} = \mathbf{0}$) and the M point is at the zone corner where the magnitude of $\boldsymbol{k}$ is greatest. (a) A "shear-unstable" packing (*i.e.* a sphere packing that is unstable at low k) at $p = 10^{-4}$ (black) and the dispersion relation for the corresponding unstressed system (blue). (b) A "$k > 0$-unstable" sphere packing (*i.e.* a packing that is stable near $k = 0$ but is unstable at higher k) at $p = 10^{-4}$ (black) and the dispersion relation for the corresponding unstressed system (blue). (c) Comparison between the lowest branch in the sphere packing (black) and its unstressed counterpart (blue) for the same system as in (b). The dashed magenta line is the difference between the two eigenvalue branches.

springs. We will use a subscript "u" (as in *e.g.*, λ_{u}) to refer to quantities corresponding to the unstressed system.

The black curves in fig. 1(a) show the six lowest eigenvalue branches, $\lambda(\boldsymbol{k})$, for a 2-dimensional packing of $N = 1024$ disks at a pressure $p = 10^{-4}$. Also shown (dashed blue curves) are the lowest eigenvalue branches for the corresponding unstressed system, $\lambda_{\mathrm{u}}(\boldsymbol{k})$, where the second term in eq. (6) has been omitted. Here, the lowest branch of the stressed system has negative curvature at $k = 0$ implying that the system has a negative shear modulus. Such shear-type instabilities have been well studied previously [8]. In the remainder of this paper, we restrict our attention to shear-stable packings that are stable near $k = 0$ but potentially unstable at higher wave vectors. We refer to this type of instability as a "$k > 0$ instability."

Figure 1(b) compares the 6 lowest eigenvalue branches of a sphere packing (black) with a $k > 0$ instability to those of its unstressed counterpart (dashed blue). The lowest branch for the sphere packing has positive curvature at $k = 0$, but becomes negative at higher k. This implies that the system is unstable to boundary perturbations corresponding to eq. (5) over a range of wavevectors. In contrast, the unstressed system, which by construction must be stable, can have only positive (or possibly zero) eigenvalues. In fig. 1(c), the dotted magenta line shows the difference between the lowest eigenvalue branch of the unstressed system (blue) and of the sphere packing (black).

The lowest eigenvalue of the unstressed system. – We estimate the eigenvalues of the packing by first evaluating the eigenvalues in the unstressed system and then considering the effect of the stress term (*i.e.* the second term in eq. (6)). In order to obtain the scaling of the $k > 0$ instabilities, we first estimate the eigenvalues at the largest wavevector, $\boldsymbol{k}_M$, *i.e.* at the M point located at the corner of the Brillouin zone. We then extend the argument to the rest of the Brillouin zone.

For the unstressed system, the lowest eigenvalue at the corner of the Brillouin zone can be estimated as follows. As fig. 1(b) suggests, the mode structure is fairly straightforward. Low-frequency vibrations are dominated by two distinct classes of modes: plane waves and the so-called "anomalous modes" that are characteristic of jammed systems [2, 4]. The lowest plane-wave branch is transverse and parabolic at low k (see fig. 1(b)): $\omega_{\mathrm{T,u}} \approx c_{\mathrm{T,u}} k$ or equivalently

$$\lambda_{\mathrm{T,u}} \approx c_{\mathrm{T,u}}^2 k^2 \sim G_{\mathrm{u}} k^2, \tag{7}$$

where G_{u} is the shear modulus of the unstressed system.

The eigenvalue of the lowest anomalous mode can be understood as follows. Wyart *et al.* [4, 5] showed that the density of vibrational states at $k = 0$ for unstressed systems, $D_{\mathrm{u}}(\omega)$, can be approximated by a step function, so that $D_{\mathrm{u}}(\omega) \approx 0$ for $\omega < \omega_{\mathrm{u}}^*$ while $D_{\mathrm{u}}(\omega) \approx$ const for $\omega > \omega_{\mathrm{u}}^*$. As suggested by fig. 1, the anomalous modes are flat in $\boldsymbol{k}$, so this is a reasonable approximation not only at $k = 0$ but over the entire Brillouin zone. Thus, the eigenvalue of the lowest anomalous mode is given by ω_{u}^* at any $\boldsymbol{k}$.

Note that if $\omega_{\mathrm{T,u}} \ll \omega_{\mathrm{u}}^*$, the lowest branch will maintain its transverse-acoustic-wave character and hence will remain parabolic in k all the way to the zone corner. However, when $\omega_{\mathrm{T,u}} \gg \omega_{\mathrm{u}}^*$, the lowest mode at the corner no longer has plane-wave character because the transverse acoustic mode will hybridize with anomalous modes and will develop the character of those modes. It follows that there is a crossover between jamming physics and plane-wave physics when $\omega_{\mathrm{T,u}} \approx \omega_{\mathrm{u}}^*$ or, equivalently, when

$$L \approx \ell_{\mathrm{T}} \equiv c_{\mathrm{T,u}}/\omega_{\mathrm{u}}^*. \tag{8}$$

Here ℓ_{T} is the transverse length identified by Silbert *et al.* [9].

Near the jamming transition, many properties scale as power laws with the excess contact number above isostaticity, $\Delta Z \equiv Z - Z^N_{\mathrm{iso}}$, where Z is the average number of contacts per particle and $Z^N_{\mathrm{iso}} = 2d\,(1-1/N) \approx 2d$. In particular, for the harmonic potentials we consider here, $\omega^*_{\mathrm{u}} \sim \Delta Z$, $G_{\mathrm{u}} \sim \Delta Z$, and $p \sim \Delta Z^2$ for dimensions $d \geq 2$. (These results are easily generalized to potentials other than the harmonic interactions used here [2].) Equation (8), in combination with eq. (7), predicts that the crossover will occur at

$$pL^4 \sim \text{const} \tag{9}$$

for $d \geq 2$.

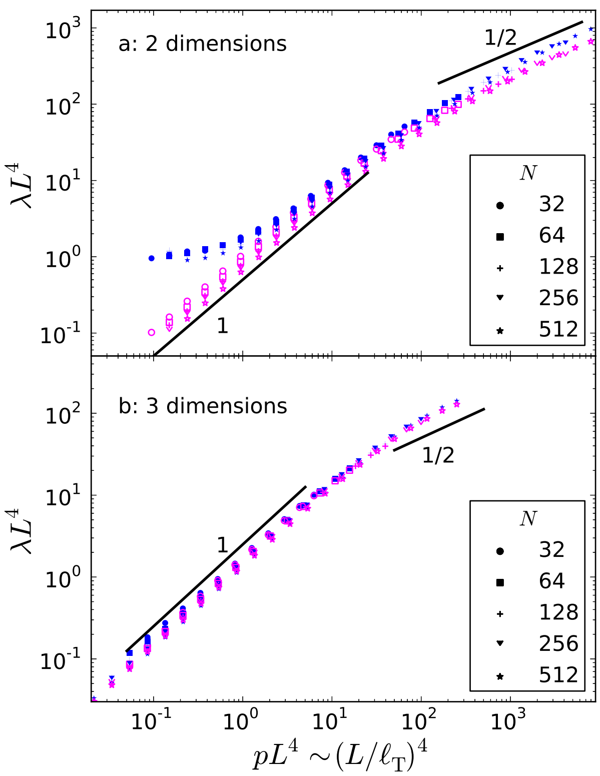

Fig. 2: The average eigenvalue of the lowest mode at the corner of the Brillouin zone of the unstressed system (blue), as well as the average difference between the unstressed system and the original packing (magenta), in (a) two and (b) three dimensions. The blue and magenta data exhibit collapse as predicted by eqs. (10) and (11), with the caveat that we were unable to reach the low pressure regime in three dimensions where we expect the scaling to be different. Data is only shown when at least 20 shear stable configurations were obtained.

A second crossover occurs at very low pressures and is due to finite-size effects that change the scaling of ΔZ to $\Delta Z \sim 1/N \sim L^{-d}$ in d dimensions, independent of p [3]. In this regime, ω^*_{u} and G_{u} remain proportional to ΔZ, and thus also scale as L^{-d} [3]. We therefore expect the lowest eigenvalue of the unstressed system at the corner of the Brillouin zone ($k_M = \sqrt{d}\pi/L$) to feature three distinct regimes.

$$\begin{aligned} \text{low pressure:}\quad \lambda_{\mathrm{u}} &\sim 1/N^2 \sim L^{-2d} \\ \text{intermediate pressure:}\quad \lambda_{\mathrm{u}} &\sim \omega^*_{\mathrm{u}} \sim p \\ \text{high pressure:}\quad \lambda_{\mathrm{u}} &\sim c_{\mathrm{T}}^2 k_M^2 \sim p^{1/2} L^{-2}. \end{aligned} \tag{10}$$

In two dimensions, we expect that $\lambda_{\mathrm{u}} L^4$ will collapse in all three regimes as a function of pL^4.

This prediction is verified in fig. 2. The blue symbols in fig. 2(a), corresponding to $\lambda_{\mathrm{u}} L^4$ of the unstressed system in $d = 2$, exhibit a plateau at low pressures/system sizes. At intermediate pL^4, the blue symbols have a slope of 1 and at high pL^4 a slope of 1/2, as predicted by eq. (10). In three dimensions (fig. 2(b)), we observe the two higher pressure regimes, with a crossover between them that scales with pL^4, as expected. We did not reach the low-pressure plateau regime in three dimensions because it is difficult to generate shear stable configurations at low pressures. Note, however, we do not expect the crossover to the low pressure regime to collapse in $d = 3$ with pL^4.

The effect of stress on the lowest eigenvalue. – With the behavior of the lowest eigenvalue of the unstressed system in hand, we now turn to the effects of stress to explore the behavior of actual sphere packings at the zone corner, $k_M = \sqrt{d}\pi/L$. The second term in eq. (6) shifts the shear modulus to smaller values without affecting the scaling with pressure, $G \sim \sqrt{p}$ [13]. It therefore follows that $G_{\mathrm{u}} - G \sim \sqrt{p}$. In the high-pressure regime, where the lowest mode is the transverse plane wave, we therefore expect that $\lambda_{\mathrm{u}} - \lambda \sim G_{\mathrm{u}} - G \sim \sqrt{p}$. Likewise, the second term in eq. (6) lowers ω^{*2}_{u} by an amount proportional to p [6,14,15], so at intermediate and low pressures it follows that $\lambda_{\mathrm{u}} - \lambda \approx \omega^{*2}_{\mathrm{u}} - \omega^{*2} \sim p$.

The difference in the lowest eigenvalues of the sphere packing and the unstressed system will therefore feature two distinct regimes:

$$\begin{aligned} \text{low and int. } p:\quad (\lambda_{\mathrm{u}} - \lambda) &\sim p \\ \text{high } p:\quad (\lambda_{\mathrm{u}} - \lambda) &\sim p^{1/2} L^{-2}. \end{aligned} \tag{11}$$

The lowest eigenvalue and stability of the original packing. – Comparing these results to eq. (10), we see that the lowest eigenvalue of the packing λ should be positive in the low pressure limit where $\lambda_{\mathrm{u}} - \lambda \ll \lambda_{\mathrm{u}}$. At high and medium pressures, λ_{u} and $\lambda_{\mathrm{u}} - \lambda$ are comparable and obey the same scaling. One would therefore expect instabilities to arise in this regime. At high pressures, however, we know that λ should be positive since $\lambda \sim G k_M^2$ and shear stability implies $G > 0$ [8]. Therefore, fluctuations about the average scaling behavior are most likely to drive the system unstable at intermediate pressures. Since this regime collapses with pressure and system size as pL^4, we expect the fraction of systems that are unstable to obey this scaling. This prediction is corroborated in fig. 3, where we see that the fraction of systems that

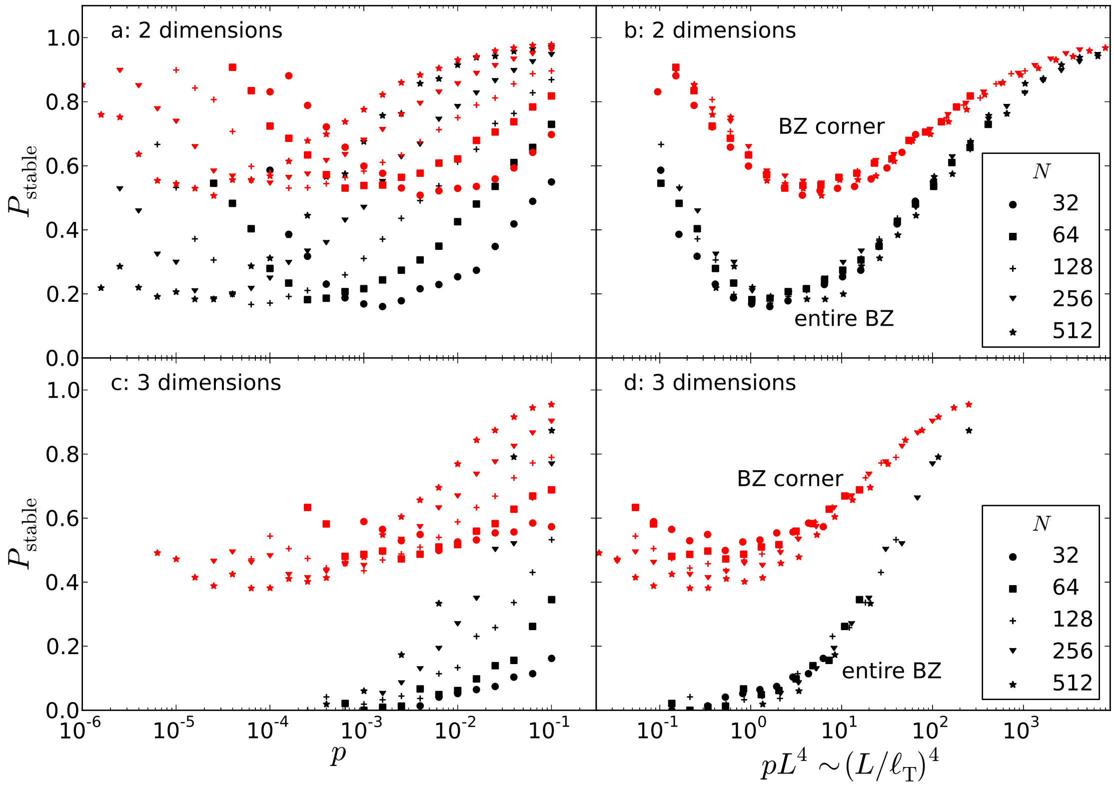

Fig. 3: The fraction of shear-stable systems in two and three dimensions that are also $k > 0$-stable. In red we plot the fraction of systems that are unstable at the M point while in black we plot the fraction of systems that are stable everywhere. We see that both collapse with pL^4, or equivalently L/ℓ_{T}, with the expected exception of the low pressure regime in three dimensions.

are stable at the M point (red data) depends on pressure p and system size L as expected.

We have thus far illustrated our reasoning for wavevectors at a zone corner, which correspond to the smallest wavelengths and thus the most drastic perturbations. Systems should therefore be more likely to go unstable at the zone corner than anywhere else. However, our arguments apply equally well to any point in the Brillouin zone.

This argument is confirmed in fig. 3. To investigate the stability over the entire zone, we computed the dispersion relation over a mesh in k space and looked for negative eigenvalues. Any configuration with a negative eigenvalue at any value of $\boldsymbol{k}$ was labeled as unstable. The black data in fig. 3 shows the fraction systems that are stable over the entire Brillouin zone. It exhibits the same qualitative features as at just the zone corner (red data), but with fewer stable configurations overall.

Discussion. – We have shown that shear stable packings can be unstable to a class of boundary perturbations that correspond to particle vibrations at non-zero $\boldsymbol{k}$. The susceptibility of packings to such perturbations is governed by the transverse length scale ℓ_{T}, which corresponds to the wavelength of the transverse plane wave with frequency ω^*; systems are stable when $L \gg \ell_{\mathrm{T}}$. Also, due to finite-size effects, there is a low-pressure regime where systems also become stable.

Note that our scaling arguments for the unstressed system apply equally well to the original packing. However, scaling alone cannot tell us the *sign* of the lowest eigenvalue. Treating the unstressed and stressed terms of the dynamical matrix separately, and exploiting the fact that the unstressed matrix is non-negative, is thus necessary for understanding the stability of the packing and emphasizes that "$k > 0$-instabilities" are caused by stress, not the geometry of the packing.

We can also consider the stability of the system to *all* infinitesimal boundary perturbations. This includes the macroscopic shear-type deformations described by Dagois-Bohy *et al.* [8] as well as those studied here. Note that any jammed packing prepared with periodic boundary conditions is stable against infinitesimal compression at all system sizes. Dagois-Bohy *et al.* [8] found that in two dimensions, the fraction of states that are shear stable collapses with pL^4 and approaches 1 at large pL^4, consistent with the speculation that the criterion for shear stability is $L \gg \ell_{\mathrm{T}}$. Here, we have shown that shear-stable packings are stable to boundary perturbations described by eq. (5) for $L \gg \ell_{\mathrm{T}}$. Moreover, the value of the lowest eigenvalue exhibits scaling collapse with L/ℓ_{T}, except at very low pressures where such scaling is expected to break down due to finite-size effects.

The combination of these two results suggests that the system should be stable to all infinitesimal boundary per-

turbations for $L \gg \ell_\mathrm{T}$. This implies that the closer the system is to the jamming transition the larger the system must be in order to be insensitive to changes in the boundaries. It also implies that the distinction between collectively and strictly jammed [7] packings disappears when $L \gg \ell_\mathrm{T}$ and thus vanishes in the thermodynamic limit for any nonzero pressure.

While the sensitivity of jammed packings to infinitesimal changes to the boundary is controlled by the diverging length scale ℓ_T, Wyart *el al.* [6] argued that the stability to a more drastic change of boundary conditions, in which the periodic boundaries are replaced with free ones, is governed by the larger length ℓ^*. Jammed packings with *free* boundaries are stable only for $L \gg \ell_\mathrm{L}$ [6]. Goodrich *et al.* [6] have shown that this length is equivalent, not only in scaling behavior but also in physical meaning, to the longitudinal length $\ell_\mathrm{L} = \omega^*/c_\mathrm{L}$ that was proposed alongside ℓ_T by Silbert *et al.* [9] and is the wavelength of the *longitudinal* plane wave with frequency ω^*.

The two length scales $\ell^* = \ell_\mathrm{L}$ and ℓ_T represent the stability of jammed packings to different classes of boundary changes and are both related to the competition between plane-wave physics and jamming physics, in that both are related to the characteristic frequency ω^* via the appropriate sound speed. The two lengths can therefore be viewed as central to the theory of the jamming transition.

To understand why some boundary perturbations are controlled by ℓ_T while others are controlled by ℓ_L, we must understand the nature of the transverse and longitudinal deformations allowed. In the case of systems with free boundaries, the system size of ℓ_L needed to support compression is also sufficient to support shear since $\ell_\mathrm{L} > \ell_\mathrm{T}$. The minimum system size needed to support both is therefore ℓ_L. In the case of periodic boundaries, we have shown here that jammed systems are stable to transverse perturbations for sizes larger than ℓ_T. However, they are stable to longitudinal perturbations at any system size. The minimum system size needed to support both is therefore ℓ_T.

The same reasoning can be applied to understanding the stability with respect to a change from periodic to fixed boundary conditions. In that case, neither longitudinal nor transverse deformations are allowed and it follows that systems of any size will be stable to this change. Mailman and Chakraborty [16] have studied systems with fixed boundary conditions to calculate point-to-set correlations. Their analysis, as well as arguments based on the entropy of mechanically stable packings, reveal a correlation length that scales like ℓ^*.

The fact that the diverging length scales control the response to boundary changes but do not enter into the finite-size scaling of quantities such as the contact number and shear modulus [3] is consistent with the behavior of a system that is at or above its upper critical dimension. The fact that power-law exponents do not depend on dimensionality for $d \geq 2$ is also consistent with this interpretation [1, 17]. However, critical systems are generally controlled by only one diverging length scale. Jamming is thus a rare example of a phase transition that displays two equally important diverging length scales. It remains to be seen whether other diverging lengths that have been reported near the jamming transition [1,16,18–20] can also be associated with boundary effects.

We thank David L. Johnson for prompting us to study vibrations of jammed tilings, Justin Burton for suggestions regarding energy minimization methods, as well as Tom Lubensky and Anton Souslov for stimulating discussions. This research was supported by the U.S. Department of Energy, Office of Basic Energy Sciences, Division of Materials Sciences and Engineering under Award DE-FG02-05ER46199 (AJL,SS,OK) and DE-FG02-03ER46088 (SN,OK), and by the NSF via the graduate research fellowship program (CPG) and the UPenn MRSEC DMR11-20901 (SS).

REFERENCES

[1] O'Hern C. S., Silbert L. E., Liu A. J. and Nagel S. R., *Phys. Rev. E.*, **68** (2003) 011306.
[2] Liu A. J. and Nagel S. R., *Annu. Rev. Condens. Matter Phys.*, **1** (2010) 347.
[3] Goodrich C. P., Liu A. J. and Nagel S. R., *Phys. Rev. Lett.*, **109** (2012) 095704.
[4] Wyart M., Nagel S. R. and Witten T. A., *Europhys. Lett.*, **72 (3)** (2005) 486.
[5] Wyart M., Silbert L. E., Nagel S. R. and Witten T. A., *Phys. Rev. E.*, **72** (2005) 051306.
[6] Goodrich C. P., Ellenbroek W. G. and Liu A. J., arXiv:1301.6981 [**cond-mat.soft**].
[7] Torquato S. and Stillinger F. H., *J. Phys. Chem. B*, **105** (2001) 11849.
[8] Dagois-Bohy S., Tighe B. P., Simon J., Henkes S. and van Hecke M., *Phys. Rev. Lett.*, **109** (2012) 095703.
[9] Silbert L. E., Liu A. J. and Nagel S. R., *Phys. Rev. Lett.*, **95** (2005) 098301.
[10] Bitzek E., Koskinen P., Gähler F., Moseler M. and Gumbsch P., *Phys. Rev. Lett.*, **97** (2006) 170201.
[11] Silbert L. E., Liu A. J. and Nagel S. R., *Phys. Rev. E*, **79** (2009) 021308.
[12] Alexander S., *Physics Reports*, **296** (1998) 65.
[13] Ellenbroek W. G., Zeravcic Z., van Saarloos W. and van Hecke M., *Europhys. Lett.*, **87** (2009) 34004.
[14] Wyart, M., *Ann. Phys. Fr.*, **30** (2005) 1.
[15] Xu N., Wyart M., Liu A. J. and Nagel S. R., *Phys. Rev. Lett.*, **98** (2007) 175502.
[16] Mailman M. and Chakraborty B., *J. Stat. Mech.*, **2011** (2011) L07002.
[17] Parisi G. and Zamponi F., *Rev. Mod. Phys.*, **82** (2010) 789.
[18] Drocco J. A., Hastings M. B., Reichhardt C. J. O. and Reichhardt C., *Phys. Rev. Lett.*, **95** (2005) 088001.
[19] Olsson P. and Teitel S., *Phys. Rev. Lett.*, **99** (2007) 178001.
[20] Vågberg D., Valdez-Balderas D., Moore M., Olsson P. and Teitel S., *Phys. Rev. E*, **83** (2011) 030303.